

Study of Influence of Hydraulic Thermoelectric Generator Resistance on Gasoline Engine Efficiency

D.O. Onishchenko, S.A. Pankratov, A.A. Zotov, A.S. Osipkov and R.A. Poshekhonov

*Bauman Moscow State Technical University,
5/1, ul. Baumanskaya 2-ya, 105005, Moscow, Russia.*

Abstract

The research covers the relevant task of increasing the piston spark-ignition engine efficiency ratio by transforming heat energy of exhaust gases into electric energy by means of a thermoelectric generator. We have studied how hydraulic resistance of the thermoelectric generator flow channel influences the engine crankshaft power for different engine operation conditions. There are linear and quadratic approximating power decrease functions of exhaust resistance derived for these conditions. A crankshaft power decrease dependence on thermoelectric generator resistance and crankshaft speed is offered. Solid Works Flow Simulation CFD software suite was used to simulate a thermoelectric generator in conditions corresponding to different engine operation conditions. The engine was simulated in operation together with a thermoelectric generator. It was shown that its application allows increasing power and decreasing fuel flow of the engine.

The TEG was simulated in conditions corresponding to different engine operation conditions and the engine was simulated in operation together with a TEG. It was shown that TEG application on a car engine allows for decreasing fuel flow by 2.02 to 2.47% based on the conditions. A bigger decrease in flow percentage can be observed for low speed crankshaft conditions.

Keywords: TEG, engine, exhaust gas energy utilization, thermoelectric generator.

INTRODUCTION

One of the main tasks set before the researchers is to increase the engine efficiency. Heat losses in combustion of fuel consume up to 71% of energy. About a half of the loss is heat removed by means of the cooling fluid and another half is heat removed in exhaust gases. A relevant way of increasing the power unit efficiency is utilizing energy of exhaust gases.

An advanced method of such utilization is installing a thermoelectric generator (TEG) in the ICE exhaust system to enable transformation of heat energy of exhaust gases immediately into electric energy [1-4, 13-17]. The principle of TEG operation is based on Seebeck effect, which makes it free of moving parts, enables highly reliable and noiseless operation. At present, such devices are being developed for gasoline engines of cars. The use of TEG allows up to 5% fuel savings [1]. In addition, thermoelectric generator can be used in order to decrease temperature upstream of a turbine for advanced engines with partial heat insulation of combustion chamber [5].

The proper selection of design solutions, parameters and operation conditions for TEG in its development is rather a difficult task, as it requires many physical processes and quality indicators to be considered: influence of gas dynamics in the flow channel, heat

conductivity in the generator housing, thermoelectric effects, and ICE operation conditions.

It is necessary to consider that alongside with producing useful electric power out of heat of exhaust gases, a TEG installed on a vehicle may negatively affect the engine operation while the TEG itself will spend some energy to maintain operation of its cooling system operation [18] and control electronics.

This study focuses on how thermoelectric generator flow channel hydraulic resistance influences the ICE performance. We evaluate power losses and increase in fuel consumption, at those operation conditions where the engine power loss exceeds TEG output electric power leads to the TEG overheating or catalyst temperature becomes insufficient to enable the operation and the exhaust gases have to bypass the TEG.

METHODS

TEG engine operation was simulated using Diesel-RK software package [6]. Resulting values of flow (G) and temperature (T) of exhaust gases were used in SW Flow Simulation software [7] to calculate electric power produced by TEG and TEG flow channel hydraulic resistance (Δp). Then, the process of operation was simulated in order to obtain fuel consumption $BSFC_{\Delta p}$ and engine power $N_{b\Delta p}$ for the engine having exhaust resistance Δp (Figure 1). The obtained data was used to determine N_{bTEG} and $BSFC_{bTEG}$ for the engine with TEG.

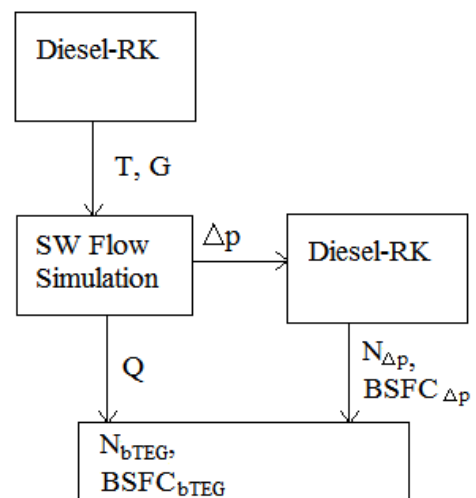


Figure 1. Flow chart of calculations

The engine chosen for the study is 4-cylinder gasoline engine VAZ 21127; bore/stroke: 75.6/82 mm/mm; compression ratio: 11.0; rated power: 106 hp (78 kW) at 5800 rpm; max. torque: 148 N·m at 4000 rpm.

Diesel-RK software is based on a zero-dimensional work flow model. Heat output of a spark-ignition engine is determined using the Vibe function (there is RK-model used for diesel engine). Mathematical model was verified using maximum power and torque data.

STUDY OF TEG RESISTANCE INFLUENCE ON ENGINE POWER

In order to determine the influence of resistance on the engine power we carried out simulation of several conditions on the full-load curve (FLC). Figure 2 shows relative decrease in the engine power ($N_{b0}-N_{b\Delta p})/N_{b0}$ as function of TEG resistance (bar) for different engine speed rpm on the FLC. There are also approximating quadratic and linear functions shown.

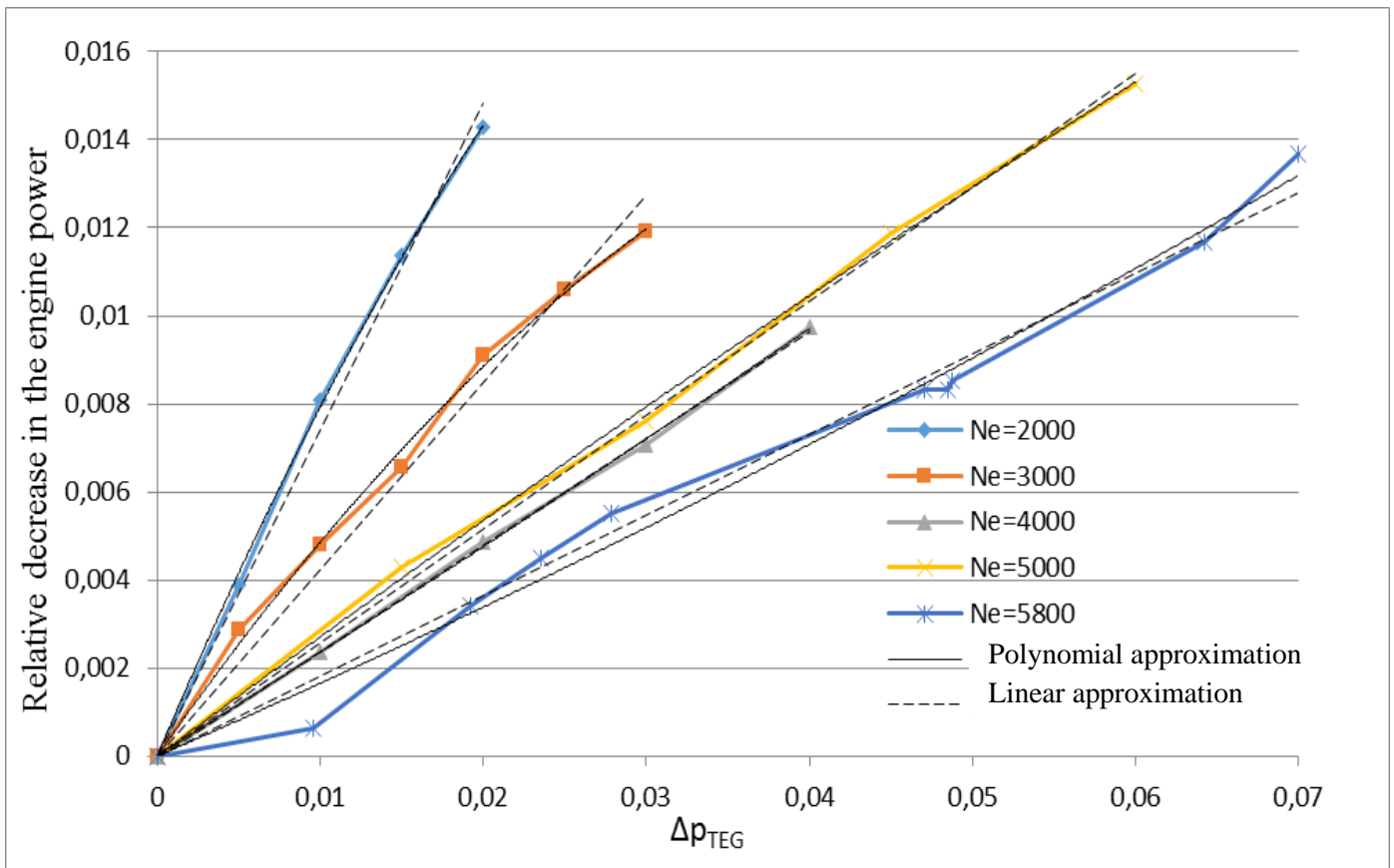


Figure 2. Loss of crankshaft power taken relative to non-TEG engine power as function of TEG resistance (bar) for different engine speed rpm on the FLC (non-TEG power is in brackets). Approximating quadratic (solid line) and linear (dashed line) functions.

The power loss dependence on the pressure drop can be represented as a linear or quadratic function that, in its turn, can be used in design or selection of TEG.

Linear approximating functions for power loss and fuel flow increase can be presented as follows:

$$N_{b0} - N_{b\Delta p} \approx p_{00} + p_{10}n + p_{01}\Delta p_{TEG} + p_{20}n^2 + p_{11}n\Delta p_{TEG}, \quad (1)$$

$$\text{where } p_{00} = 22.35, p_{10} = -0.009376, p_{01} = 0.1918, p_{20} = 9.521 \cdot 10^{-7}, p_{11} = -8.303 \cdot 10^{-6}.$$

$$\Delta q_{fuel_Lost} = q_{fuel} n_E, \Delta p_{eg} - q_{fuel} n_E, 0 = b_0 + b_{10}n_E + b_{01}\Delta p_{eg}. \quad (2)$$

$$\text{where } b_{00} = -0.003981 \text{ kg}\cdot\text{hour}^{-1}; b_{10} = 5.98e-8; b_{01} = \text{kg}\cdot\text{hour}^{-1}\cdot\text{Pa}^{-1}$$

Approximating functions determined in Matlab cftool are shown on Figure 3.

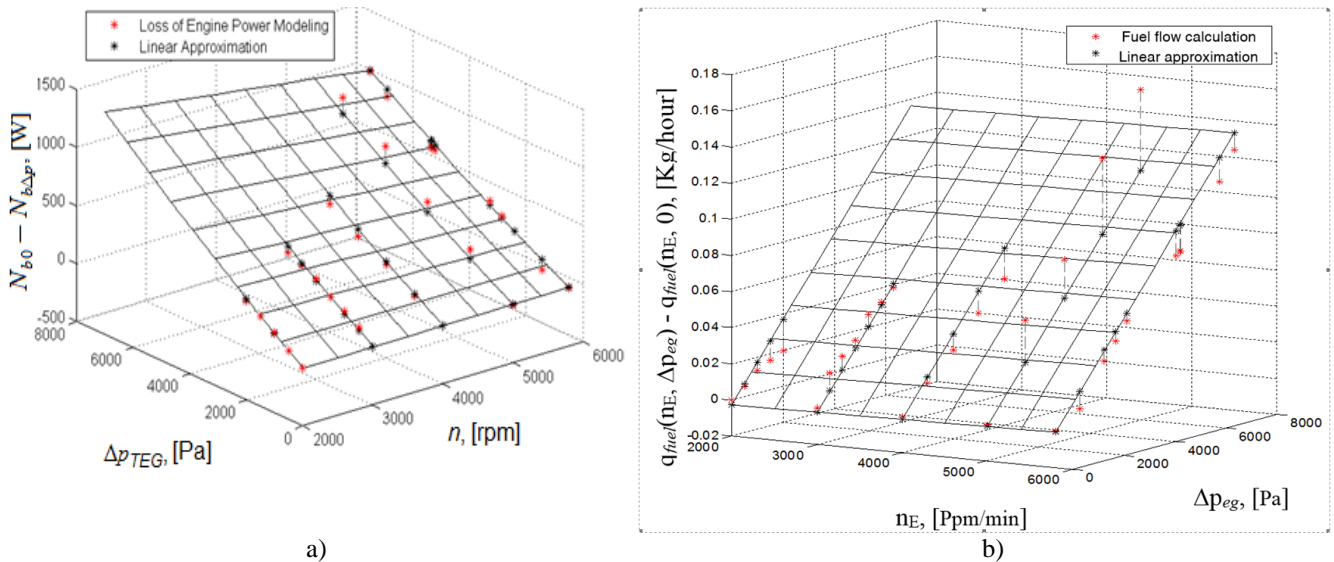


Figure 3. Approximation of the VAZ 21127 ICE power loss (a) and fuel flow (b) dependences on TEG exhaust pressure drop Δp_{eg} and ICE crankshat speed n_E at maximum power

The average relative deviation of approximation of $Q_{mech_Lost} n_E, \Delta p_{eg}$ power loss dependence on TEG exhaust pressure drop Δp_{eg} and ICE crankshat speed n **Error! Reference source not found.** is 14%.

The average relative deviation of approximations of $\Delta q_{fuel_Lost} n_E, \Delta p_{eg}$ fuel flow decrease dependence on TEG exhaust pressure drop Δp_{eg} and ICE crankshat speed n **Error! Reference source not found.** is 29%. Formally, the root-mean-square deviation could be decreased out of a higher polynomial degree and higher number of constants. But it is very undesirable as it could result in high beats in intermediate points.

The built approximating functions (Figures 3 and 4) show that decrease in power Q_{ICE} and increase in fuel flow q_{fuel} are almost in a linear dependence on TEG pressure drop Δp_{eg} but their dependence on the engine speed is not that clear. It can be explained by the zero-dimensional work flow model error and by the fact that relative changes in values are small as compared to the very values. However, the resulting approximating curves qualitatively and quantitatively represent the inverse effect of TEG flow channel hydraulic resistance on ICE power and fuel flow.

EFFICIENCY ESTIMATION OF TEG APPLICATION ON POWER UNIT IN VIEW OF ITS HYDRAULIC RESISTANCE

For the purpose of efficiency estimation, we studied the structure, as shown on Figure 4. Thermoelectric generator consists of a hot heat exchanger, thermoelectric batteries (TEB) and cold heat exchangers. The hot heat exchanger is a hexagonal chamber that receives hot exhaust gases which heat the interior wall of the hot heat exchanger. In order to intensify the heat exchange process the thermoelectric generator flow channel may be supplemented with a flow expander, plates or other elements that increase the heat exchange area and gas turbulization. This study covers a hot heat exchanger with variable height fins that equalize the temperature of the thermoelectric batteries. Heat flow passes from the hot heat exchanger through the thermoelectric battery to cooling fluid via the cold heat exchanger. The thermoelectric battery transforms heat energy into electric energy.

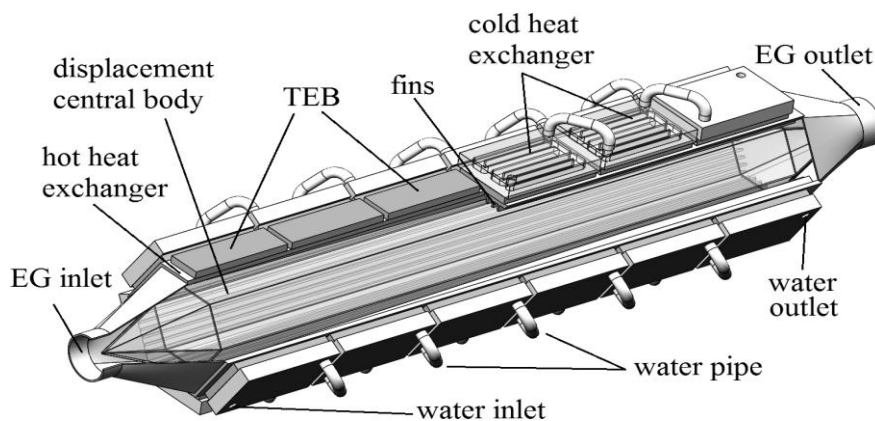


Figure 4. Diagram of thermoelectric generator

Thermal processes in the thermoelectric generator were simulated using Flow Simulation software of Solid Works package [7].

Gas motion and heat exchange are described by a set of differential Navier-Stokes equations in partial derivatives [8]. The set

comprises the following equations: equation for conservation of momentum, equation for conservation of energy and continuity equation. When written in the indicial form, the equations look as follows [9]: Navier-Stokes equation for compressible fluid:

$$\rho \frac{DW_i}{D\tau} = G_i - \frac{\partial p}{\partial x_i} + \frac{\partial}{\partial x_j} \left[\mu \left(\frac{\partial W_i}{\partial x_j} + \frac{\partial W_j}{\partial x_i} - \frac{2}{3} \delta_{ij} \frac{\partial W_k}{\partial x_k} \right) \right],$$

where $i, j, k=1, 2, 3, \delta_{ij} = \begin{cases} 0 & \text{if } i \neq j \\ 1 & \text{if } i=j \end{cases}$ - Kronecker symbol, ρ -

density, W_i - velocity vector components, G_i - bulk forces vector components.

Equation for conservation of energy:

$$\rho \frac{DH}{D\tau} + \rho W_j \frac{\partial H}{\partial x_j} = \frac{\partial}{\partial x_j} \left(\lambda \frac{\partial T}{\partial x_j} \right) + \frac{\partial p}{\partial \tau} + \frac{\partial}{\partial x_j} (\tau_{ij} W_j) + G_j W_j + w_r Q_r + \frac{\partial q_{Rj}}{\partial x_j},$$

where $H = h + \frac{W^2}{2}$ - total energy, $\frac{\partial q_{Rj}}{\partial x_j}$ - radiative heat flux, τ_{ij}

- friction induced shear stress, Q_r - quantity of heat released per unit mass from chemical reaction at rate w_r , τ -time.

Continuity equation:

$$\frac{\partial \rho}{\partial \tau} + \frac{\partial}{\partial x_i} (\rho W_i) = 0$$

Turbulent flow is described in Flow Simulation using the modified k- ϵ turbulence model (Lam-Bremhorst k- ϵ model [10]). The boundary layer is described using a two-tier model that applies two different approaches describing thin and thick boundary layers [11].

The chosen software package implements a computational solution for this set of differential equations with by the finite volume method.

Heat conductivity in TEG parts is described by Fourier's heat conductivity equation:

$$\nabla(\lambda \nabla T) + q_v = c \rho \frac{\partial T}{\partial \tau},$$

where T - temperature, c - heat capacity, q_v - power of energy internal heat sources, λ - heat conductivity.

The developed simulation model allows determining coefficients of heat transfer from gases to the hot heat exchanger and from cooling fluid to the cold heat exchanger. Besides, the model allows

determining the distribution of temperatures on the hot heat exchanger fins and gas temperature distribution lengthwise the thermoelectric generator.

In order to simulate thermoelectric modules, the model of material was developed with parameters corresponding to the thermoelectric material properties ($2.574 \text{ W} \cdot \text{m}^{-1} \text{K}^{-1}$). Heat conductivity for the cold heat exchanger is taken equal to $200 \text{ W} \cdot \text{m}^{-1} \text{K}^{-1}$ while for other parts it is equal to $43 \text{ W} \cdot \text{m}^{-1} \text{K}^{-1}$.

Cartesian mesh [12] consists of $2.9 \cdot 10^6$ cuboidal cells, including $8 \cdot 10^5$ cells for fluid modeling.

The boundary conditions set for gas: flow, temperature, and parameters of inlet turbulence (intensity and scale of turbulent fluctuations are 5% and 0.002, respectively) and outlet pressure. Flow rates and temperature for each of conditions were determined by means of zero-dimensional work flow simulation.

Water flow is $1.94 \cdot 10^{-5} \text{ kg/m}^3$ through a package of six heat exchangers, temperature is 90°C . The defined coefficient of heat transfer for the surfaces of body parts (except for the cold heat exchanger) exposed to the atmosphere is $5 \text{ W} \cdot \text{m}^{-2} \text{K}^{-1}$ (ambient temperature is 20°C).

RESULTS

The simulation results are shown on Figures 5 and 6 and in Table 1. Figure 5 shows that the temperature of batteries at downstream of the heat exchanger is higher than upstream, which speaks for the necessity of further optimizing the geometry of fins.

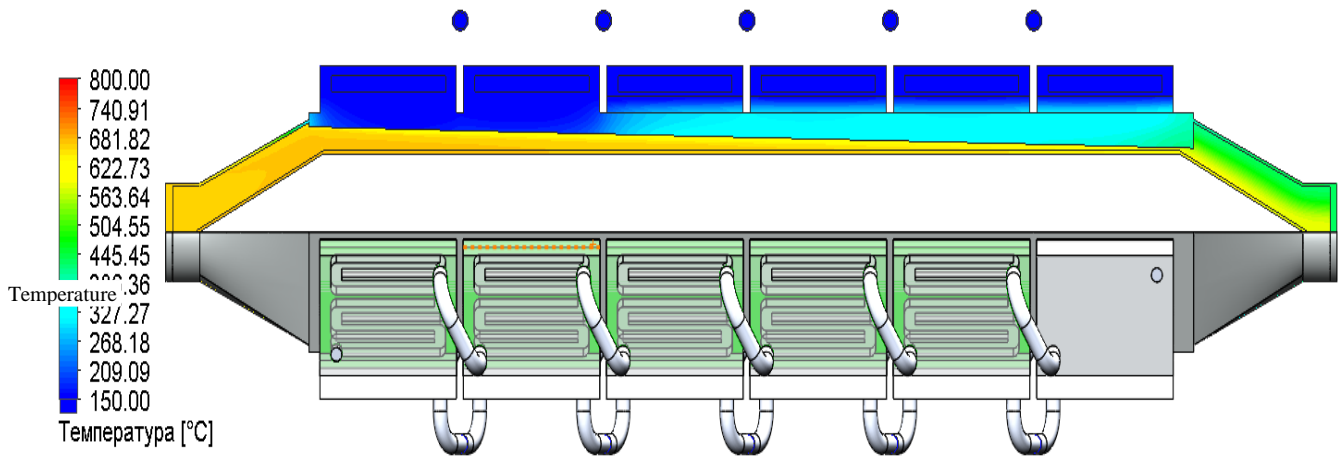


Figure 5. Results of waste gases flux modeling at rated conditions. Flow temperature, °C

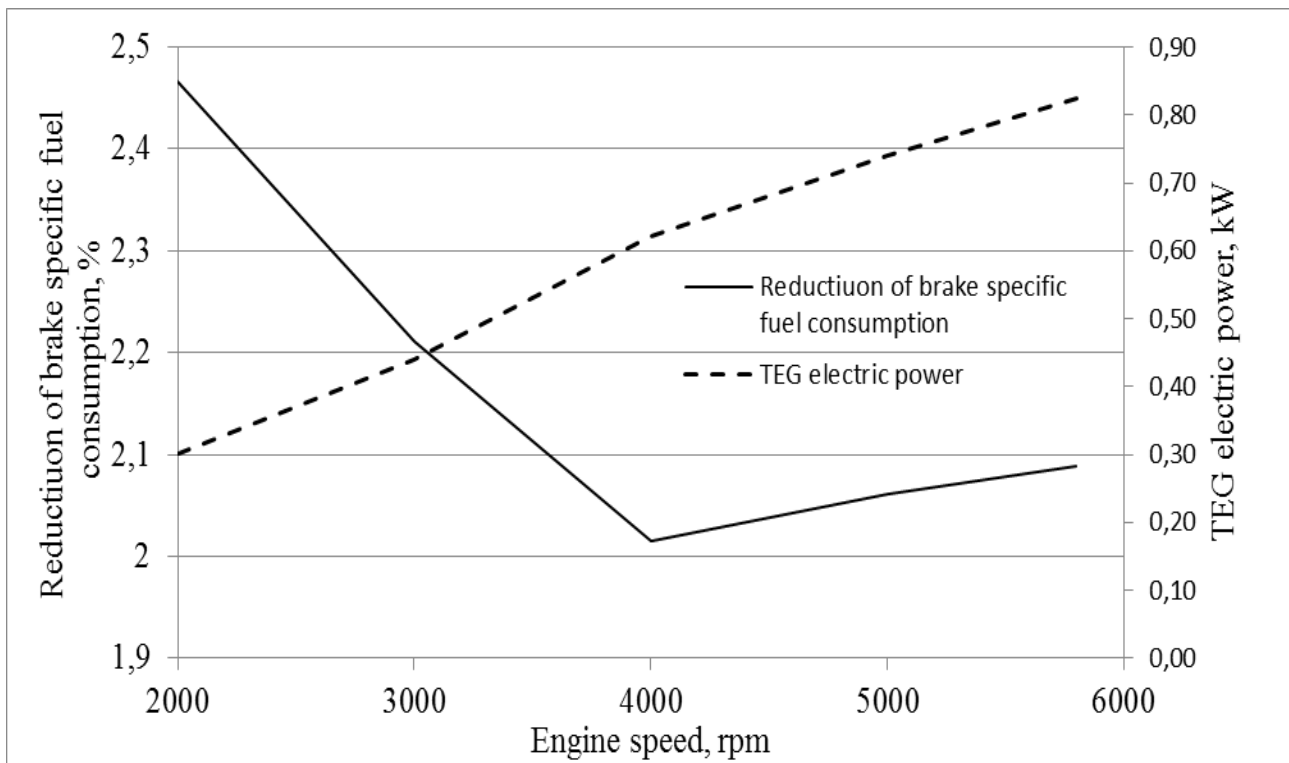


Figure 6. TEG electric power and reduction of brake specific fuel consumption vs engine speed

Based on the resulting data, we simulated an engine equipped with a thermoelectric generator. The TEG efficiency is taken equal throughout the conditions: $\eta_{TEG} = 0.05$ (here η_{TEG} accounts for thermal element losses, current converter losses, as well as losses from pumping water through the cold heat exchanger and fan drive). Evaluation of increase in power out of TEG should account for the alternator efficiency ($\eta_{alt} = 0.5$). Thus, thermoelectric generator engine power is determined as:

$$N_{bTEG} = N_{b\Delta p} + \frac{\eta_{TEG}}{\eta_{alt}} Q_{TEG} \quad (3)$$

Specific fuel consumption:

$$BSFC_{TEG} = \left(\frac{1}{BSFC_{\Delta p}} + \frac{\eta_{TEG} Q_{TEG}}{\eta_{alt} BSFC_{\Delta p} N_{b\Delta p}} \right)^{-1} \quad (4)$$

The calculation results are shown on Figure 5 and in Table 1 (Appendix).

Table 1. Simulation results

Engine speed	rpm	2000	3000	4000	5000	5800
TEG resistance Δp_{TEG}	bar	0.001115	0.0028	0.00622	0.01051	0.01345
Non-TEG engine power N_{b0}	kW	24.39	39.705	61.766	72.013	79.072
Non-TEG engine BSFC $BSFC_0$	g/(kW·h)	0.25398	0.24748	0.24968	0.24962	0.25462
Power of an engine (exhaust resistance is equal to TEG resistance $N_{b\Delta p}$)	kW	24.376	39.683	61.608	71.91	78.91
BSFC of an engine (exhaust resistance is equal to TEG resistance $N_{b\Delta p}$)	g/(kW·h)	0.25403	0.24758	0.24989	0.24991	0.25485
Power decrease $N_{b0} - N_{b\Delta p}$	kW	0.014	0.022	0.158	0.103	0.162
EG temperature upstream TEG	K	822	874.00	928.00	926.00	936.60
EG temperature downstream TEG	K	590.00	663.00	733.00	744.00	756.00
EG temperature reduction on TEG	K	232.00	211.00	195.00	182.00	175.60
EG mass flux	kg/s	0.02578	0.04092	0.0619	0.07987	0.08915
TEG cooling	kW	6.01	8.77	12.42	14.82	16.48
TEG electric power	kW	0.30	0.44	0.62	0.74	0.82
TEG engine power N_{bTEG}	kW	40.56	62.85	73.39	80.56	24.98
Power increase $N_{bTEG} - N_{b0}$	kW	0.59	0.86	1.08	1.38	1.49
	%	2.41	2.15	1.75	1.91	1.88
Fuel flow decrease $BSFC_0 - BSFC_{TEG}$	g/(kW·h)	0.2479	0.2422	0.2450	0.2449	0.2496
	%	2.466	2.211	2.015	2.061	2.088

DISCUSSION

The figure and table show that TEG application throughout the FLC conditions allows decreasing fuel flow by 2.02-2.47%; a higher decrease in fuel flow percentage can be observed for low crankshaft speed conditions. The engine power loss because of TEG exhaust resistance is negligibly small as compared to the engine power; however, this value is of the same magnitude as TEG power.

It should be noted that the simulation applies to the one specific design of generator with longitudinal fins of variable height in hot heat exchanger. A TEG producing higher electric power can be developed for the engine in question out of an increase in heat transfer from exhaust gases. At the same time, such generator would probably create a higher hydraulic resistance, which would result in loss of power and additional fuel consumption. Besides, it may appear that in some conditions TEG power consumption and ICE power loss because of the generator can exceed the useful electric power produced from heat of exhaust gases.

Linear functions (1) and (2) and linear power function of exhaust resistance will be also valid for engines of different make while the specific engine simulation is required to obtain the proper coefficients.

CONCLUSIONS

1. We have studied how the TEG exhaust resistance influences the engine crankshaft power for different engine operation conditions on the full-load curve. There are linear and quadratic approximating power decrease functions of exhaust resistance derived for each of these conditions.
2. The dependence of crankshaft power decrease and fuel flow increase on thermoelectric generator exhaust resistance and crankshaft speed is offered. The TEG influence on the engine can be simulated using both zero-dimensional work flow simulation and approximating functions.
3. The TEG was simulated in conditions corresponding to different engine operation conditions and the engine was simulated in operation together with a TEG. It was shown that TEG application on a car engine allows for decreasing fuel flow by 2.02 to 2.47% based on the conditions. A bigger decrease in flow percentage can be observed for low speed crankshaft conditions.
4. Development of a thermoelectric generator of efficient design calls for resolving the optimization problem. Generators of different design may appear to be efficient for different types and conditions of

ICEs. In view of the fact that these conditions are constantly changing while a vehicle is moving, the optimum TEG design should provide for a variable geometry of the hot heat-exchanger.

ACKNOWLEDGEMENTS

The research work was supported by the Ministry of Education and Science of the Russian Federation (grant #14.577.21.0113, unique identifier RFMEFI57714X0113).

CONVENTIONAL SYMBOLS AND ABBREVIATIONS:

n – engine speed;
 n_{max} – rated engine speed;
 N_{b0} – brake power (non-TEG engine);
 $N_{b\Delta p}$ – power of an engine which exhaust resistance is equal to the TEG resistance;
 N_{bTEG} – brake power (TEG engine);
 $BSFC_0$ – Brake specific fuel consumption (non-TEG engine);
 $BSFC_{TEG}$ – Brake specific fuel consumption (TEG engine)
 $BSFC_{AP}$ – Brake specific fuel consumption (with the exhaust resistance equal to the TEG resistance)
 M_b – brake torque;
 Δp_{TEG} – hydraulic resistance of TEG flow channel;
 p_{amb} – ambient pressure;
TEG – thermoelectric generator;
TEB – thermoelectric battery;
EG – exhaust gases;
 η_{alt} – alternator efficiency;
 η_{TEG} – TEG efficiency;
FLC – full-load curve;
PCE – power conversion efficiency

REFERENCES

- [1] S. Kumar, S. Heister, X. Xu, J. Salvador, G. Meisner, "Thermoelectric Generators for Automotive Waste Heat Recovery Systems Part I: Numerical Modeling and Baseline Model Analysis," *Journal of Electronic Materials*, vol. 42, no. 4, 665–674, 2013.
- [2] A.I. Leontiev, R.Z. Kavtaradze, D.O. Onishchenko, A.S. Golosov, S.A. Pankratov, "Improvement of piston engine operation efficiency by direct conversion of the heat of exhaust gases into electric energy," *High Temperature*, vol. 54, no. 1, 104 – 111, 2016.
- [3] J. Liebl, S. Neugebauer, A. Eder, M. Linde, B. Mazar, W. Stütz, "The Thermoelectric Generator from BMW is Making Use of Waste Heat," *MTZ*, vol. 70, 4-11, 2009.
- [4] S. Risse, H. Zellbeck, "Close-coupled exhaust gas energy recovery in a gasoline engine," *MTZ*, vol. 74, 54-61, 2013.
- [5] A.I. Leontiev, D.O. Onishchenko, S.A. Pankratov, A.Yu. Smirnov, "Use of the Thermoelectric Generator for the Turbine Efficiency of a Diesel Engine with a Partial Insulation of the Combustion Chamber," *Teplovye processy v tehnikе [Heating Processes in Technics]*, Issue 5, 227-232, 2016.
- [6] The program DIESEL-RK. Date Views 30.12.2016. <http://www.diesel-rk.bmstu.ru>.
- [7] SOLIDWORKS Flow Simulation. Date Views 30.12.2016. <https://www.solidworks.com/sw/products/simulation/flow-simulation.htm>
- [8] G.N. Abramovich, "Prikladnaja gazovaja dinamika" [Applied Gas Dynamics], 5th Issue, Nauka, Moscow, 1991.
- [9] R.Z. Kavtaradze, D.O. Onishchenko, A.A. Zelentsov, "Trehmernoe modelirovanie nestacionarnyh teplofizicheskikh processov v porshnevnyh dvigateljah: uchebnoe posobie" [Three-Dimensional Simulation of Transient Thermophysical Processes in Piston Engines: Textbook], Bauman Moscow State Technical University, Moscow, 2012.
- [10] C.K.G. Lam, K.A. Bremhorst, "Modified Form of the k-ε Model for Predicting Wall Turbulence," *Journal of Fluids Engineering*, vol. 103, 456-460, 1981.
- [11] Enhanced turbulence modeling in Solidworks flow simulation. Dassaultsystemes, Solidworks corporation, Waltham, USA, 2013.
- [12] Advanced boundary Cartesian meshing technology in Solidworks Flow simulation. Dassaultsystemes, Solidworks corporation, Waltham, USA, 2013.
- [13] A.S. Osipkov, R.A. Poshekhonov, M.O. Makeev, S.A. Pankratov, G.A. Arutyunyan, A.O. Basov, R.A. Safonov, "Effectiveness of thermoelectric generators mounted into exhaust tract of internal combustion engine," *Book of abstracts 14th European Conference on Thermoelectrics (ECT2016)*, Lisbon, Portugal, p. 165, 2016. http://www.itn.pt/ect2016-conference/ECT2016_Book_Abstracts_With_Org_Comm_LO.PDF Visited 20.10.2016
- [14] L.E. Bell, "Cooling, Heating, Generating Power, and Recovering Waste Heat with Thermoelectric Systems," *Science*, vol. 321, no. 5895, 1457-1461, 2008.
- [15] J. Yang, "Potential applications of thermoelectric waste heat recovery in the automotive industry," *IEEE 24th International Conference on Thermoelectrics*, Clemson, South Carolina, pp. 170-174, 2005.
- [16] M.A. Karri, E.F. Thacher, B.T. Helenbrook, "Exhaust energy conversion by thermoelectric generator: Two case studies," *Energy Conversion and Management*, vo. 52, no. 3, 1596–1611, 2011.
- [17] D.M. Rowe, "Thermoelectrics Handbook: Macro to Nano," CRC Press, 1014 p., 2005.
- [18] M.A. Korzhuev, "Concerning a conflict between internal combustion engines and thermoelectric generators in heat recovery in cars," *Pis'ma v zhurnal tehnikeskoj fiziki [Letters in Technical Physics Journal]*, vol. 37, no. 4, 151-153, 2011.